

Alkoxyamines of Stable Aromatic Nitroxides: N–O vs. C–O Bond Homolysis

by **Didier Gigmes**^{*a}), **Anouk Gaudel-Siri**^b), **Sylvain R. A. Marque**^a), **Denis Bertin**^a), **Paul Tordo**^a), **Paola Astolff**^c), **Lucedio Greci**^{*c}), and **Corrado Rizzoli**^d)

^a) UMR 6517 case 542, Université de Provence, Avenue Escadrille Normandie-Niemen, F-13397 Marseille Cedex 20 (fax: +33-4-91-28-87-58; e-mail: didier.gigmes@up.univ-mrs.fr)

^b) UMR-CNRS 6178, Université Paul Cézanne/Aix-Marseille, Faculté des Sciences et Techniques, Case D12, F-13397 Marseille Cedex 20

^c) Dipartimento di Scienze dei Materiali e della Terra, Università Politecnica delle Marche, via Brecce Bianche, I-60131 Ancona (fax: +39-071-2204714; e-mail: l.greci@univpm.it)

^d) Dipartimento di Chimica Generale ed Inorganica, Chimica Analitica, Chimica Fisica, Università, viale G. P. Usberti, I-43100 Parma

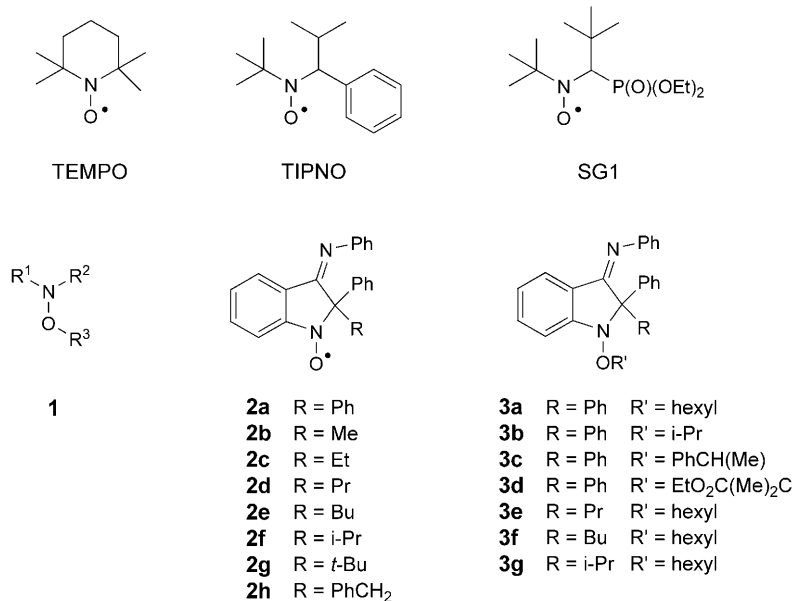
Dedicated to the memory of Professor *Hanns Fischer*

A series of stable 2,2-disubstituted 3-(phenylimino)indol-1-oxyls, the alkoxyamines **3**, were prepared, characterized, and tested as possible candidates in controlled radical polymerization (CRP). The structures of **3d** and **10** were additionally solved by X-ray diffraction. The lability of the N–O(C) and (N)O–C bonds of compounds **3** were compared, and the possibility of N–O vs. O–C bond cleavage was evaluated by thermal degradation, ESR spin trapping, MS experiments, and DFT calculations. Alkoxyamines with a primary- or secondary-alkyl group bound to the O-atom of the nitroxide function (hexyl and *i*-Pr) mainly underwent (undesired) N–O bond homolysis. When the *O*-alkyl radical was a tertiary or a benzyl group (crotonyl or styryl), O–C bond cleavage occurred as the main process, thus suggesting a possible use of these compounds in CRP processes.

1. Introduction. – Two decades ago, *Rizzardo* and co-workers [1], as well as *Georges et al.* [2] showed that it is possible to prepare well-defined polymers by using nitroxyl radicals or alkoxyamines as catalysts. Nitroxide-mediated polymerization (NMP) was, thus, born [3][4], and it inspired several studies with the aim to understand the mechanism [5] and kinetics of polymerization [6–11], to prepare new polymers [3][12–14], and to develop more-efficient initiators/controllers [15–22].

Among the few commercially available nitroxides, TEMPO (=2,2,6,6-tetramethylpiperidinoxy radical) has been widely used, although it proved to be efficient only in the polymerization of styrene derivatives [23]. To overcome this limitation, the synthesis of new nitroxides has been developed. The use of TEMPO-based nitroxides and, above all, of acyclic nitroxides having a H-atom on one of the α -C-atoms, such as TIPNO [17] and SG1 [24], and their corresponding alkoxyamines **1**, represents a breakthrough in the field of NMP. After the development of these new nitroxide radicals, it is now possible to polymerize acrylates, acrylamides, 1,3-dienes, and acrylonitrile monomers [23] with accurate control.

Up to now, the major drawback of NMP has been the difficulty in controlling the polymerization of methacrylate derivatives [25]: livingness and control could be

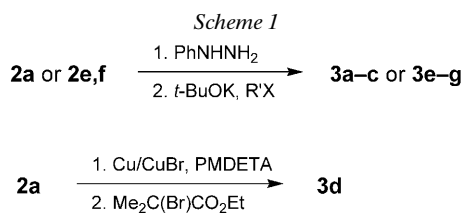


reached only in the presence of a small amount of co-monomer [26]. Recently, we overcame this limitation by using alkoxyamines based on DPAIO (**2a**) nitroxides, which allowed us to control the polymerization of methyl methacrylate at 100°, with 60% conversion [27]. Compound **2a** belongs to the family of ‘indolinonic nitroxides’ [28], aromatic nitroxides with the nitroxide function being in conjugation with the benzene ring. Usually, these radical species are more stable than tetramethylpiperidino- and tetramethylpyrrolidino derivatives. In particular, nitroxides **2a–c** do not significantly decompose when heated at 200° in *Dowtherm* solution [29]. Compounds **2f–h** are less stable due to the easy elimination of alkyl radicals (*i*-Pr, *t*-Bu, Bn) from the C-atom in position 2 [28]. The nitroxides **2g** and **2h** have a low thermal stability, and they decompose even at 100°.

To evaluate the efficiency of these nitroxides in NMP, the alkoxyamines **3a–d** were synthesized by alkylation of **2a**, which is one of the most stable compounds among the above selection. In particular, compound **3a** was synthesized to study its activity in the polymerization of ethylene (=ethene) [30], which is normally carried out at 250° under a pressure of 2000 atmospheres. The alkoxyamine **3d** was designed for the controlled polymerization of methyl methacrylate. Finally, the alkoxyamines **3e–g** were synthesized from **2d–f**, respectively, to ascertain the role, if any, of the alkyl group at C(2).

2. Results. – 2.1. *Synthesis.* The alkoxyamines **3a–g** (with the exception of **3d**) were prepared from the nitroxides **2a**, **2e**, and **2f**, which were reduced *in situ* with phenylhydrazine in the presence of a stoichiometric amount of potassium *tert*-butoxide (*t*BuOK) to give the corresponding hydroxylamine anions (*Scheme 1*). Addition of the appropriate alkyl halide to these anions led to the formation of the desired alkoxyamines **3**. Compound **3d** was easily prepared from **2a** according to the atom-transfer radical-addi-

tion (ATRA) method [31] using the corresponding activated bromide in the presence of Cu^{I} and a small amount of Cu^{0} (Scheme 1). In all cases, the yields were very high, ranging from 80 to 91% (see *Exper. Part*).



The alkoxyamines **3a–g** were identified on the basis of their spectroscopic data. Both the IR and $^1\text{H-NMR}$ spectra were very similar for all the compounds synthesized. In particular, the IR spectra showed two characteristic bands typical of the indoline structures [32], one at *ca.* 1650 cm^{-1} for the $\text{C}=\text{N}$ group, the other, the so-called *Witkop* band, at *ca.* 1595 cm^{-1} for the Ph-N-(OR)-C group. Compound **3d** showed an additional IR band at 1732 cm^{-1} for the $\text{C}=\text{O}$ group. In the $^1\text{H-NMR}$ spectra, as expected, the same pattern was evident for the aromatic H-atoms of each alkoxyamine. However, compounds **3b** and **3c** did not show well-resolved peaks for the Me groups, most likely due to hindered rotation of the alkyl group about the N-O-R bonds.

2.2. *X-Ray Crystallographic Analyses.* 2.2.1. *Structure of 3d.* The bond distances and angles in **3d** were as expected (see *Table 1* and *Fig. 1*). The distance $\text{N}(2)\text{-C}(2)$ (1.270 \AA) and the $\text{C}(2)\text{-N}(2)\text{-C}(13)$ angle (120.0°) are in agreement with the interaction of a double bond. The indoline ring is not planar, with maximum deviations from planarity of $-0.240(3)$ and $0.222(2)\text{ \AA}$ for $\text{C}(1)$ and $\text{N}(1)$, respectively. The three Ph rings ($\text{C}(13)$ to $\text{C}(18)$, $\text{C}(19)$ to $\text{C}(25)$, and $\text{C}(25)$ to $\text{C}(30)$) form with the mean plane of the indoline ring dihedral angles of 81.4 , 89.2 , and 76.7° , respectively. *Van der Waals* interactions are the main contacts among the molecules in the crystal. The two intermolecular interactions between $\text{O}(2)$, $\text{N}(2)$, and C-H of two Ph rings may be interpreted as weak H-bonds: *a*) $\text{C}(16)\cdots\text{O}(2)^{\text{i}}$, $3.581(3)\text{ \AA}$; $\text{H}(16)\cdots\text{O}(2)^{\text{i}}$, 2.72 \AA ; $\text{C}(16)\text{-H}(16)\cdots\text{O}(2)^{\text{i}}$, 154.2° ; *b*) $\text{C}(29)\cdots\text{N}(2)^{\text{ii}}$, $3.676(4)\text{ \AA}$; $\text{H}(29)\cdots\text{N}(2)^{\text{ii}}$, 2.81 \AA ; $\text{C}(29)\text{-H}(29)\cdots\text{N}(2)^{\text{ii}}$, 155.2° ($\text{i}=1+x, y, 1+z$; $\text{ii}=1.5-x, -y, -0.5+z$).

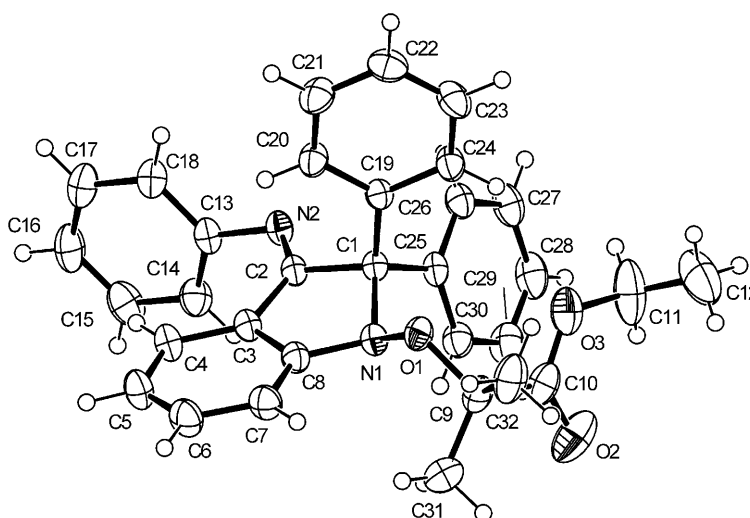
2.2.2. *Structure of 10.* The structure of **10** (see below) could also be solved by X-ray crystallography (*Fig. 2*). Bond distances and angles again fell in the expected range (*Table 1*). The indoline ring is approximately planar, with maximum deviations from planarity of -0.092 and 0.071 \AA for $\text{C}(2)$ and $\text{N}(1)$, respectively. The dihedral angles formed by the Ph rings ($\text{C}(9)$ to $\text{C}(14)$, $\text{C}(15)$ to $\text{C}(20)$, and $\text{C}(21)$ to $\text{C}(26)$) with the mean plane of the indoline ring are 86.9 , 88.4 , and 68.5° , respectively. Two weak $\text{C-H}\cdots\text{N}$ intramolecular H-bond interactions are observed: *a*) $\text{C}(22)\cdots\text{N}(1)$, 2.795 \AA ; $\text{H}(22)\cdots\text{N}(1)$, 2.43 \AA ; $\text{C}(22)\text{-H}(22)\cdots\text{N}(1)$, 103.5° ; *b*) $\text{C}(26)\cdots\text{N}(2)$, 3.028 \AA ; $\text{H}(26)\cdots\text{N}(2)$, 2.60 \AA ; $\text{C}(26)\text{-H}(26)\cdots\text{N}(2)$, 108.9° .

Here, the crystal packing is mainly determined by *Van der Waals* contacts.

2.3. *Mass Spectrometry.* The mass spectra of compounds **3a–d** were very significant, the fragmentation pattern depending on the nature of the *O*-alkyl group. In fact, **3a** and **3b** (both having a primary *O*-alkyl group) showed very low intensities of the molecular-

Table 1. Selected Bond Distances (in Å) and Angles (in °) for **3d** and **10**

3d			
O(1)–N(1)	1.432(2)	N(1)–O(1)–C(9)	113.0(1)
O(1)–C(9)	1.459(2)	C(10)–O(3)–C(11)	118.8(2)
O(2)–C(10)	1.195(4)	O(1)–N(1)–C(1)	113.3(1)
O(3)–C(10)	1.320(3)	O(1)–N(1)–C(8)	112.1(1)
O(3)–C(11)	1.468(4)	C(1)–N(1)–C(8)	107.0(1)
N(1)–C(1)	1.512(3)	C(2)–N(2)–C(13)	120.0(2)
N(1)–C(8)	1.414(3)		
N(2)–C(2)	1.270(3)		
N(2)–C(13)	1.419(2)		
10			
O(1)–C(7)	1.374(5)	C(7)–O(1)–C(27)	116.6(3)
O(1)–C(27)	1.425(5)	C(1)–N(1)–C(8)	109.1(3)
N(1)–C(1)	1.486(5)	C(2)–N(2)–C(9)	120.8(3)
N(1)–C(8)	1.386(5)		
N(2)–C(2)	1.259(5)		
N(2)–C(9)	1.411(5)		

Fig. 1. X-Ray crystal structure of **3d**. ORTEP View (40%-probability ellipsoids).

ion peak in their mass spectra, the most important peak in both cases appearing at m/z 359, which corresponds to the fragment originating from the parent alkoxyamine after loss of an hexyloxy or an isopropyloxy group, respectively. Compounds **3c** and **3d** gave mass spectra in which the molecular-ion peaks were clearly visible. Other well-defined peaks were found at m/z 375 and 359, corresponding to the fragments derived from the cleavage of the O–C and N–O bonds of the alkoxyamine moiety, respectively (see below).

2.4. ESR Spin-Trapping Experiments and Thermal Stability of **3a–g**. The stability of the nitroxides **2a–h** has already been described [29]. The data reported in the literature

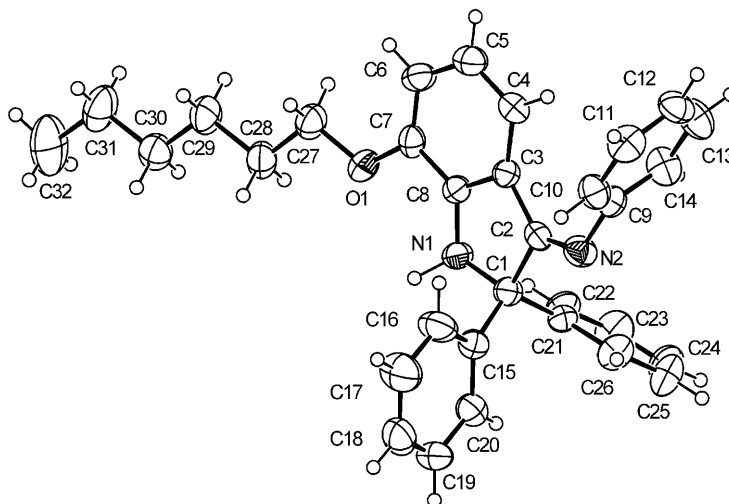


Fig. 2. X-Ray crystal structure of **10**. ORTEP View (40%-probability ellipsoids).

indicate that the thermal stability of these nitroxides depends on the nature of the substituent R at C(2) of the indole moiety. The higher the stabilization of the radical R, the lower the stability of the nitroxide. For this reason, **2g** and **2h** having a *t*-Bu and a Bn group at C(2), respectively, are less stable and decompose at temperatures $<100^\circ$. Nitroxide **2a**, in which two Ph groups are present at C(2), is very stable, similar as nitroxides with a primary alkyl group at C(2). For this reason, we focused our attention on alkoxyamines derived from **2a**.

To gain information on the stabilities of the alkoxyamines **3a–d**, their benzene solutions were heated at 80° directly inside the ESR cavity, and the identification of alkyl or alkoxy radicals eventually formed was achieved by means of the spin-trapping technique, with ‘*tert*-butyl- α -phenylnitronne’ (PBN, **4**)¹⁾ being used as the spin trap. Thermal decomposition may occur according to two different pathways (*Scheme 2*).

The radical adduct formed from the trapping of the aminyl radical **6** by PBN (**4**) was not detected because it is thermally unstable and, if formed, would have rapidly decomposed. In addition, its formation could be inhibited by crowding around the radical center. The different radical species generated during the thermal decomposition of **3a–d** in the presence of PBN (**4**) were identified from the experimental ESR spectra with the aid of computer simulations [33]. The results are summarized in *Table 2*.

From *Table 2*, it is clear that different radical adducts were formed (in different ratios) from the various alkoxyamines depending on the nature of the alkyl group R'. In particular, the ESR spectrum of **3a** (not shown) was found to be the superposition of two different signals in a 95 : 5 ratio, one corresponding to that of the nitroxide **7a**, the other belonging to the acyl nitroxide **8**, respectively.

¹⁾ Systematic name: *N*-(1,1-dimethylethyl)-*N*-(phenylmethylidene)amine oxide.

Scheme 2

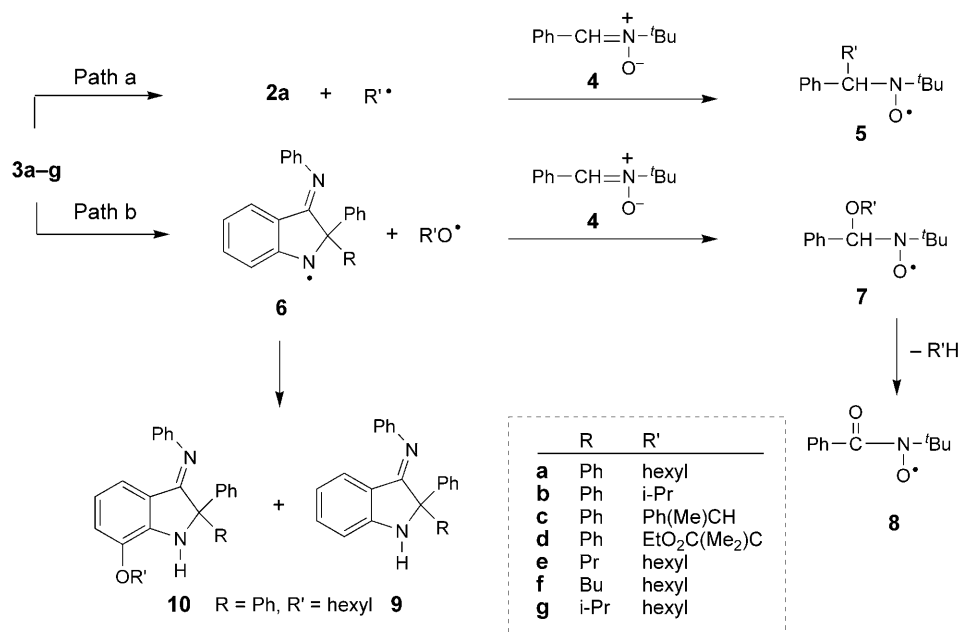


Table 2. Product Distribution (in %) of the Different Radical Species Observed by ESR During Thermal Decomposition of Alkoxyamines **3**. Conditions: in benzene solution for 40 min at 80° in the presence of PBN (**4**).

Starting material	2a	5	7	8
3a	–	–	95	5
3b	–	–	92	8
3c	43	15	–	42
3d	79	7	14	–
3d^a	60	40	–	–

^a) After 10 min of heating.

The same radical adducts were obtained from the thermal decomposition of compound **3b** in the presence of PBN (**4**), and in fact, nitroxides **7b** and **8** were obtained in a 92 : 8 ratio, respectively (Fig. 3). Simulation of the experimental spectrum recorded from alkoxyamine **3c** was in agreement with the superposition of three different signals due to nitroxides **2a**, **5c**, and **8** (Fig. 4). A similar behavior was observed for compound **3d**: after 40 min of heating, a composite spectrum exhibiting the signals of nitroxides **2a**, **5d**, and **7d** in a ratio of 79 : 7 : 14, respectively, was recorded (not shown). In this last case, after 10 min of heating, a spectrum was formed only by the signal of **2a** and **5d** (Fig. 5). The hyperfine-coupling constants of the formed nitroxides are collected in Table 3. Note that compounds **3e–g**, when heated at 80°, behave like compound **3a**.

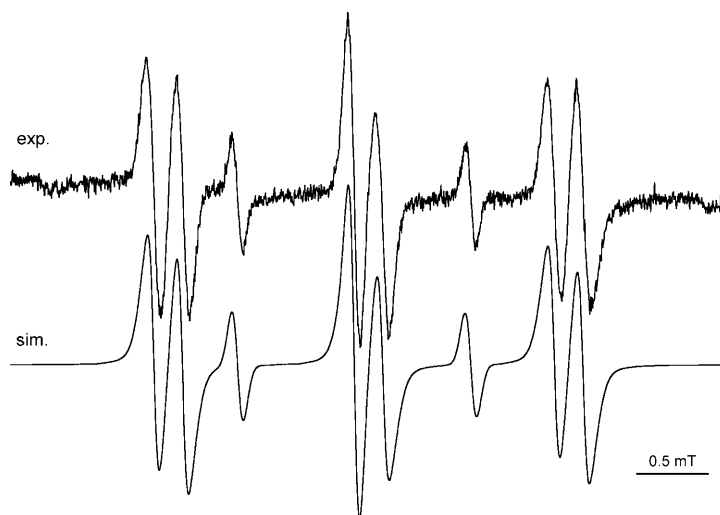


Fig. 3. Experimental (exp.) vs. simulated (sim.) ESR spectra for the radical adducts formed in the thermal decomposition of **3b** in the presence of PBN (**4**) after 40 min at 80°

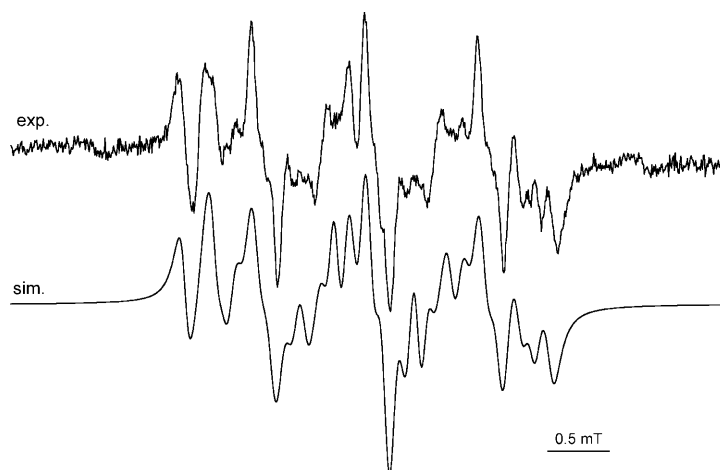


Fig. 4. Experimental (exp.) vs. simulated (sim.) ESR spectra for the radical adducts formed in the thermal decomposition of **3c** in the presence of PBN (**4**) after 40 min at 80°

2.5. Preparative-Scale Thermal Decomposition. Compound **3a** was thermally decomposed on a preparative scale by heating a *tert*-butylbenzene solution of the alkoxyamine under reflux for 1.5 h. In agreement with the ESR spin-trapping experiment, DPAIO was not formed, and compound **9** (70%) was the main product, together with **10** (30%).

2.6. Bond-Dissociation-Enthalpy (BDE) Calculations. The BDE values for the alkoxyamines **3a–d** were calculated to compare the lability of the corresponding N–

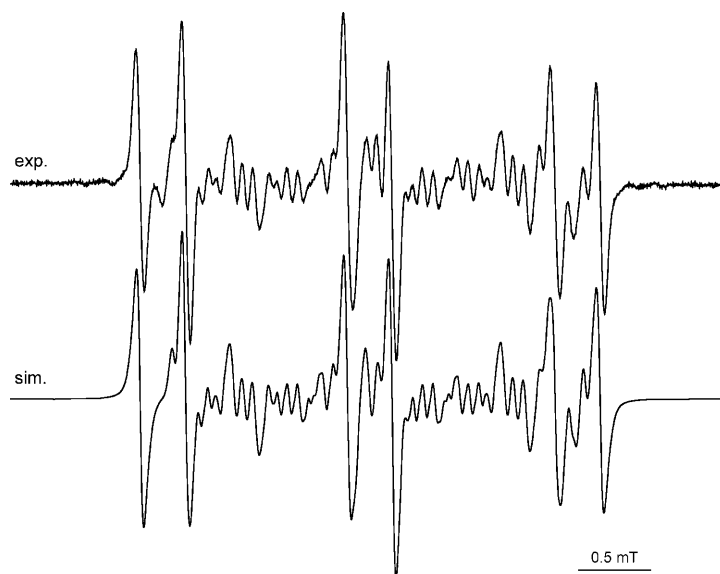


Fig. 5. Experimental (exp.) vs. simulated (sim.) ESR spectra for the radical adducts formed in the thermal decomposition of **3d** in the presence of PBN (**4**) after 10 min at 80°

Table 3. ESR Hyperfine Coupling Constants (in mT) for Selected Compounds. Conditions: in benzene at 80° (see Exper. Part).

Radical	$a(\text{N})$	$a(\text{H})$
2a ^{a)}	0.943	–
5d	1.443	0.313
7a	1.405	0.229
7d	1.393	0.203
7c	1.400	0.232
8	0.811	–

^{a)} Values for other atoms: $a_{\text{H}(5)} = 0.314$, $a_{\text{H}(7)} = 0.303$, $a_{\text{H}(4)} = a_{\text{H}(6)} = 0.104$, $a_{\text{N}(\text{exo})} = 0.072$.

O(C) and (N)O–C bonds. The BDEs for the two competitive pathways at 298 K are defined by Eqns. 1 and 2:

$$\text{BDE}_{\text{C-O}} = \Delta H_{\text{f}}^{\circ}(\text{nitroxide}) + \Delta H_{\text{f}}^{\circ}(\text{R}^{\bullet}) - \Delta H_{\text{f}}^{\circ}(\text{N-alkoxyamine}) \quad (1)$$

$$\text{BDE}_{\text{N-O}} = \Delta H_{\text{f}}^{\circ}(\text{aminyl}) + \Delta H_{\text{f}}^{\circ}(\text{RO}^{\bullet}) - \Delta H_{\text{f}}^{\circ}(\text{N-alkoxyamine}) \quad (2)$$

Density-functional-theory (DFT) calculations were performed with the Gaussian03 software package [34]. Recently [35][36], various standard functionals have been tested to calculate BDE values of C–X and X–Y bonds belonging to a large panel of compounds. The best results were obtained with the B3P86 functional, and the best correlation constants between the experimental and calculated values were

obtained at the B3P86/6-311++G(d,p)//B3LYP/6-31G(d) level. Herein, the geometry optimization and the calculation of vibrational frequencies were performed at the B3LYP/6-31G(d) level, and a single point at the B3P86/6-311++G(d,p) level was used to calculate the energy. All minima were confirmed by a calculation of vibrational frequencies. For thermodynamic calculations, as recommended by Wong [37], a scale factor of 0.9804 was applied to the vibrational frequencies. The BDEs were then calculated according to Eqn. 3 (for $T=298$ K):

$$\text{BDE} = \Delta H_{\text{r}}^{\circ} = D_{\text{e}} + \Delta(\text{ZPE}) + \Delta H_{\text{trl}} + \Delta H_{\text{rot}} + \Delta H_{\text{vib}} + RT \quad (3)$$

Here, D_{e} is the classical electronic bond-dissociation energy, $\Delta(\text{ZPE})$ is the difference in zero-point energy between the products and the *N*-alkoxyamine, and ΔH_{trl} , ΔH_{rot} , and ΔH_{vib} are the contributions from translational, rotational, and vibrational degrees of freedom, respectively. The results of these studies are reported in Table 4.

Table 4. Comparison of the Bond-Dissociation Enthalpies (BDE) for the (N)O–C vs. N–O(C) Cleavage of **3** at 298 K. All values calculated at the B3P86/6-311++G(d,p)//B3LYP/6-31G(d) level.

Compound	BDE [kJ mol ⁻¹]	
	(N)O–C	N–O(C)
3a	175	136
3b	173	141
3c	118	137
3d	102	126

3. Discussion. – According to the experiments carried out on the thermal decomposition of **3a–d**, as described above, it is clear that the pathway followed in the thermal homolysis is related to the nature of the R' group. When R' is a nonstabilized alkyl group, as in **3a,b**, the bond-dissociation enthalpy (BDE) for the N–O(C) bond is lower than that for the (N)O–C bond. When R' is a stabilized substituent, the BDEs for the two bonds are closer to each other, as in the case of **3c**. For compound **3d**, the BDE for the (N)O–C bond is smaller than for N–O(C). These data are in agreement with those obtained from the MS analyses of the different alkoxyamines (see above). In fact, the most-important mass peaks in the spectra of all studied compounds (with the exception of **3c** and **3d**) are due to the aminyl radical **6** formed from the starting alkoxyamine after N–O(C) bond cleavage, with loss of the *O*-alkyl moiety. This result is also supported by the thermal-decomposition experiment. When **3a** was refluxed in *tert*-butylbenzene, no DPAIO was recovered, and the main product isolated corresponded to **9** (70%) derived from the aminyl fragment **6**. The second product, compound **10**, was also formed *via* the intermediate aminyl radical. Compounds **3c** and **3d**, *i.e.*, *O*-styryl and *O*-methylcrotonate, showed in their mass spectra both the peaks of the nitroxide **2a** and of the aminyl fragment **6** (R=Ph), the latter being less intense than that of the nitroxide in the case of **3d**.

The thermal decomposition of **3a–d** at 80° in the presence of PBN (**4**) inside the ESR cavity were also convincing. With the exception of **3c** and **3d**, the spectra recorded during the decomposition of all the other alkoxyamines correspond to the *O*-alkyl–

PBN spin adduct **7** and to the acyl nitroxide **8**, its thermal decomposition product (see *Fig. 3*). In the case of **3c** and **3d**, the ESR spectrum of **2a** was also detected, thus indicating that O–C bond cleavage occurs. In particular, in the case of **3d**, the spin adduct **5d** was observed (see *Fig. 5*). The spin adducts **5** and **7** were identified on the basis of the hyperfine coupling for the α -H-atom, which should be *ca.* 0.3 mT when an alkyl group is attached to the same C-atom, and *ca.* 0.2 mT when an alkoxy group is present [38].

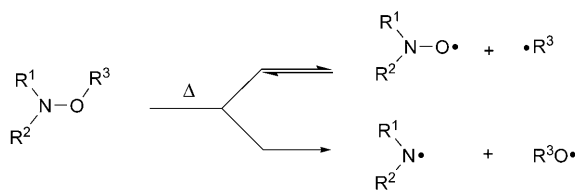
The above data may be rationalized by the observation that N–O(C) bond cleavage easily occurs because of the formation of the resonance-stabilized aminyl radical **6**; however, when the radical bonded to the O-atom in these aromatic nitroxides is sufficiently stabilized, as in the case of styryl and methyl crotonate-1-yl, the cleavage of the O–C bond also occurs (**3c** and **3d**). With **3d**, (N)O–C cleavage is favored compare to **3c** due to an increase of the steric hindrance of the released alkyl fragment. Compared to **3a** and **3b**, the (N)O–C cleavage of **3c** is the main process due to both increased steric hindrance and stabilization of the released alkyl part; DFT calculations support these experimental results (*Table 4*). In fact, the calculated BDE_{N-O} values are quite constant ($\Delta BDE_{N-O} = 19 \text{ kJ mol}^{-1}$), while the calculated BDE_{O-C} values are strongly influenced by the nature of the substituents attached to the C-atom ($\Delta BDE_{O-C} = 73 \text{ kJ mol}^{-1}$).

For **3a** and **3b**, the BDE_{N-O} values are significantly lower than the BDE_{O-C} ones (ΔBDE *ca.* 35 kJ mol^{-1}), and in fact, amine and alkoxy radicals are formed, being the sole products observed. In the case of **3c** and **3d**, the (N)O–C bond is the most labile, and its homolysis is favored with respect to N–O(C) homolysis. This can be rationalized by the released radical being stabilized by π -electron delocalization, whereas the parent alkoxyamine is destabilized by steric hindrance. As already pointed out [35], the combination of both steric and electron-withdrawing effects for the released radical (**3d**) leads to a significant decrease in the BDE_{O-C} value. For **3c,d**, a small gap (*ca.* 20 kJ mol^{-1}) between BDE_{O-C} and BDE_{N-O} was observed, which justifies the detection of both aminyl and nitroxyl radicals in the ESR spin-trapping experiments. The gap between the BDE values for the two different bonds is larger for **3d**, with BDE_{O-C} being considerably lower than BDE_{N-O} , and, indeed, a higher ratio of nitroxyl/aminyl radicals was detected.

Introduction of an alkyl group, *i.e.*, Pr, i-Pr, or Bu on C(2) of the indole ring, as in alkoxyamines **3e–g**, does not affect the behavior of these compounds. As in the case of **3a**, during their thermal decomposition, the aminyl radical was mainly formed, which suggests that, for the studied compound, it is the nature of the group attached to the O-atom of the nitroxide function that determines the particular kind of homolysis, *i.e.*, N–O(C) *vs.* (N)O–C cleavage, with no influence by the other groups present on the indole ring.

4. Conclusions. – During our investigation on the use of DPAIO alkoxyamines in NMP, we discovered that the thermal decomposition may occur in two different ways (*Scheme 3*). Thereby, there may be a competition between (N)O–C and N–O(C) bond cleavage. The possibility and the extent of bond cleavage depend on the nature of the alkyl moiety R^3 bound to the O-atom of the nitroxide function, as deduced by detailed studies of the thermal decomposition of the alkoxyamines **3a–d** by means of ESR spin-trapping experiments, MS analyses, laboratory-scale experiments, and DFT calculations.

Scheme 3



It is obvious that, except for **3d**, the studied alkoxyamines **3** are not suitable to mediate controlled radical polymerization since their thermal decomposition occurs predominantly between the N–O(C) bond. However this alkoxyamines can afford an interesting way to produce alkoxy radicals at medium-to-high temperatures. In a forthcoming paper, we will present a successful living controlled radical polymerization of a different substrate (MMA) using **3d**-type initiators/controllers [27].

University of Provence and CNRS are kindly acknowledged for financial support.

Experimental Part

1. *General*. The nitroxides **2a–h** were prepared starting from 2-phenyl-3-phenylimino-3H-indole *N*-oxide [39] according to a procedure reported previously [28]. Solvents and chemicals were purchased from *Carlo Erba* and *Sigma-Aldrich* and used as received. Melting points (m.p.) were measured with an electrothermal apparatus; uncorrected. IR Spectra: *Perkin-Elmer Spectrum MGXI* spectrophotometer equipped with a Spectra Tech ‘Collector’ for DRIFT measurements; in cm^{-1} . $^1\text{H-NMR}$ Spectra: *Varian Gemini-200* spectrometer; at r.t. in CDCl_3 soln.; δ in ppm rel. to Me_4Si , Δ in Hz. ESR Spectra: upgraded *Bruker ER-200D* spectrometer. GC/MS: *Carlo Erba QMD-1000* mass spectrometer equipped with a *Fisons GC-8060* chromatograph; in *m/z*.

2. *Synthesis of 3a–c and 3e–g* (General Procedure). To a soln. of **2a** (1 mmol) and the appropriate alkyl halide (6 mmol) in THF (10 ml) was added phenylhydrazine (1 mmol) under Ar gas. Upon reduction, the color changed from red to yellowish. Then, $^t\text{BuOK}$ (2 mmol) was added, and the mixture was stirred at r.t. for 1 h. The mixture was diluted with Et_2O (25 ml) and washed with dist. H_2O (3×20 ml). The org. phase was dried (Na_2SO_4) and evaporated, and the residue was crystallized from the appropriate solvent (see below).

N-[1-(Hexyloxy)-1,2-dihydro-2,2-diphenyl-3H-indol-3-ylidene]aniline (**3a**). Yield: 89%. M.p. $85\text{--}86^\circ$ (ligroin, b.p. $40\text{--}60^\circ$). IR: 1652 (C=N), 1596 (Ph–N(O–hexyl)–C). $^1\text{H-NMR}$ (200 MHz, CDCl_3): 0.86 (unresolved *t*, 3 H); 1.20–1.25 (*m*, 6 H); 1.48–1.62 (*m*, 2 H); 3.85 (*t*, $J=6.8$, 2 H); 6.40 (*d*, $J=6.8$, 1 H); 6.62 (*t*, $J=7.2$, 1 H); 6.79 (*d*, $J=7.2$, 2 H); 7.05–7.15 (*m*, 2 H); 7.27–7.36 (*m*, 10 H); 7.51–7.56 (*m*, 3 H). EI-MS (pos.): 461 (2.5, $[M+1]^+$), 375 (5), 361 (30), 359 (100), 283 (18), 254 (14), 205 (26) 165 (39), 152 (44). Anal. calc. for $\text{C}_{32}\text{H}_{32}\text{N}_2\text{O}$: C 83.44, H 7.0, N 6.08; found: C 84.47, H 7.04, N 6.12.

N-[1,2-Dihydro-1-[(1-methylethyl)oxy]-2,2-diphenyl-3H-indol-3-ylidene]aniline (**3b**). Yield: 90%. M.p. $152\text{--}153^\circ$ (ligroin, b.p. $60\text{--}100^\circ$). IR: 1657 (C=N), 1596 (Ph–N(O i Pr)–C). $^1\text{H-NMR}$ (200 MHz, CDCl_3): 1.17 (br. *s*, 6 H); 3.93 (*sept.*, 1 H); 6.40 (*d*, $J=7.8$, 1 H); 6.61 (*t*, $J=7.2$, 1 H); 6.79 (*d*, $J=7.2$, 2 H); 7.08–7.13 (2 arom. H); 7.28–7.34 (9 arom H); 7.50–7.59 (br. *s*, 4 H). EI-MS (pos.): 418 (1.3, M^+), 375 (1.2), 361 (30), 360 (100), 2.81 (7), 254 (8), 205 (18). Anal. calc. for $\text{C}_{29}\text{H}_{26}\text{N}_2\text{O}$: C 83.22, H 6.26, N 6.69; found: C 83.14, H 6.22, N 6.71.

N-[1,2-Dihydro-2,2-diphenyl-1-[(1-phenylethyl)oxy]-3H-indol-3-ylidene]aniline (**3c**). Yield: 91%. M.p. $162\text{--}163^\circ$ (benzene/petroleum ether). IR: 1657 (C=N), 1596 (Ph–N(O–styryl)–C). $^1\text{H-NMR}$ (200 MHz, CDCl_3): 1.36 (br. *s.*, 3 H); 4.61 (*q*, $J=7.8$, 1 H); 6.34 (*d*, $J=8.9$, 1 H); 6.55 (*t*, $J=7.8$, 1 H);

7.03–7.38 (*m*, 15 H); 7.53–7.65 (*m*, 4 H); 7.73 (*d*, $J=7.8$, 2 H). EI-MS (pos.): 480 (7, M^+), 376 (27), 375 (30), 362 (17), 360 (52), 299 (38), 285 (23), 284 (100), 205 (33), 165 (19). Anal. calc. for $C_{34}H_{28}N_2O$: C 84.97, H 5.87, N 5.83, found: C 84.95, H 5.91, N 5.87.

N-[1-(Hexyloxy)-1,2-dihydro-2-phenyl-2-propyl-3H-indol-3-ylidene]aniline (**3e**). M.p. 64–66° (ligroin, b.p. 60–100°). IR: 1661(C=N), 1598(Ph–N(OPr)–C). 1H -NMR (200 MHz, $CDCl_3$): 0.87 (*t*, $J=6$, 3 H); 0.98 (*t*, $J=6$, 3 H); 1.15–1.56 (*m*, 12 H); 2.43 (*m*, 1 H); 2.51–2.61 (*m*, 1 H); 3.71–3.79 (*m*, 1 H); 3.83–3.90 (*m*, 1 H); 6.34 (*d*, $J=9$, 1 H); 6.57 (*t*, $J=9$, 1 H); 6.77 (*d*, $J=9$, 2 H) 7.05–7.10 (*m*, 2 H); 7.23–7.35 (*m*, 6 H); 7.52 (*d*, $J=9$, 2 H). EI-MS (pos.): 426 (3, M^+), 325 (100), 283 (17). Anal. calc. for $C_{29}H_{34}N_2O$: C 81.43, H 8.86, N 6.40; found: C 81.65, H 8.83, N 6.57.

N-[2-Butyl-1-(hexyloxy)-1,2-dihydro-2-phenyl-3H-indol-3-ylidene]aniline (**3f**). M.p. 44–45° (ligroin, b.p. 60–100°). IR: 1661(C=N), 1597(Ph–N(OBu)–C). 1H -NMR (200 MHz, $CDCl_3$): 0.87 (*t*, $J=6$, 3 H); 0.92 (*t*, $J=6$, 3 H); 1.16–1.42 (*m*, 10 H); 1.52–1.64 (*m*, 2 H); 2.35–2.45 (*m*, 1 H); 2.54–2.63 (*m*, 1 H); 3.73–3.80 (*m*, 1 H); 3.84–3.91 (*m*, 1 H); 6.35 (*t*, $J=9$, 1 H); 6.58 (*t*, $J=6$, 1 H); 6.77 (*d*, $J=6$, 2 H); 7.05–7.11 (*m*, 2 H); 7.23–7.35 (*m*, 6 H); 7.51 (*d*, $J=6$, 2 H). EI-MS (pos.): 440 (10, M^+), 384 (13), 340 (100), 295 (45), 283 (39). Anal. calc. for $C_{30}H_{36}N_2O$: C 81.78, H 8.24, N 6.36; found: C 81.97, H 8.36, N 6.15.

N-[1-(Hexyloxy)-1,2-dihydro-2-(1-methylethyl)-2-phenyl-3H-indol-3-ylidene]aniline (**3g**). M.p. 109–110° (ligroin, b.p. 60–100°). IR: 1667(C=N), 1597 (Ph–N(OⁱPr)–C). 1H -NMR (200 MHz, $CDCl_3$): 0.90 (*t*, $J=6$, 3 H); 1.07 (*t*, $J=6$, 3 H); 1.15 (*d*, $J=6$, 3 H); 1.25–1.45 (*m*, 6 H); 1.61–1.70 (*m*, 2 H); 3.15–3.29 (*t*, $J=6$, 1 H); 3.91–4.08 (*m*, 2 H); 6.31 (*d*, $J=9$, 1 H); 6.52 (*t*, $J=9$, 1 H); 6.78 (*d*, $J=9$, 2 H); 7.02–7.11 (*m*, 2 H); 7.25–7.31 (*m*, 6 H); 7.60 (*d*, $J=9$, 2 H). EI-MS (pos.): 426 (9, M^+), 383 (86), 325 (100), 299 (62), 282 (75). Anal. calc. for $C_{29}H_{34}N_2O$: C 81.43, H 8.86, N 6.40; found: C 81.49, H 8.78, N 6.53.

The Nitroxides **2d–f** were transformed into the corresponding hexyl-substituted compounds **8e–g** as reported for compounds **3a–c**.

3. *Synthesis of Ethyl 2-[[2,3-Dihydro-2,2-diphenyl-3-(phenylimino)-1H-indol-1-yl]oxy]-2-methylpropanoate (3d)*. Compound **2a** (1 mmol) and ethyl 2-bromoisobutyrate (2 mmol) were dissolved in anhyd. toluene (5 ml) in a 50-ml round-bottom flask, and degassed with Ar. In another 50-ml flask, Cu (2 mmol) and CuBr (2 mmol) were suspended in anhyd. toluene (5 ml), degassed for 10 min with Ar, and then treated with pentamethyl-diethylenetriamine (PMDTA; 1 mmol), and finally degassed again for another 10 min. Next, the content of the first flask was poured into that of the second under Ar atmosphere. The resulting reaction mixture was stirred for 30 min and then diluted with Et_2O (60 ml). The org. layer was washed with H_2O (3×20 ml), dried (Na_2SO_4), and evaporated. The residue was purified by column chromatography (CC) (SiO_2 ; petroleum ether/ Et_2O 9:1) and recrystallized from ligroin. Yield of **3d**: 80%. M.p. 106–107° (ligroin, b.p. 60–100°). IR: 1732 (C=O), 1660 (C=N), 1594 (Ph–N(OCMe₂CO₂Et)–C). 1H -NMR (200 MHz, $CDCl_3$): 1.19 (*t*, $J=7.5$, 3 H); 1.32 (*s*, 6 H); 3.88 (br. *s*, 2 H); 6.4 (*d*, $J=7.5$, 1 H); 6.67 (*t*, $J=7.5$, 1 H); 6.78 (*d*, $J=8.2$, 2 H); 7.03–7.14 (*q*-like, 1 H); 7.28–7.33 (*m*, 10 H); 7.41 (br. *s*, 4 H). EI-MS (pos.): 490 (8, M^+), 375 (45), 360 (13), 299 (11), 283 (40), 205 (18), 165 (18), 78 (100). Anal. calc. for $C_{32}H_{30}N_2O_3$: C 78.34, H 6.16, N 5.71; found: C 78.39, H 7.62, N 5.76. X-Ray crystal structure: see Fig. 1, Exper. 6.1, and Table 5.

4. *ESR Measurements*. A soln. of the appropriate compound **3** (2 mg) and PBN (**4**; 2 mg) in anhyd. benzene (1 ml) was transferred to an ESR tube, accurately degassed by bubbling with Ar gas, and heated at 80°. The final spectra resulted from ten accumulations in 40 min. Computer-simulated ESR spectra were calculated with the WinSim program in the NIEHS public ESR software-tools package (see <http://www.epr.niehs.nih.gov/>) [33].

5. *Thermal Decomposition of 3a*. Compound **3a** (100 mg) was heated at 160° in 5 ml of *tert*-butylbenzene for 1.5 h. After this time, the reaction soln. was reduced to a small volume (*ca.* 1 ml) and then subjected to prep. TLC (SiO_2 ; cyclohexane/AcOEt 95:5). Compound **9** was obtained in 70% yield, together with **10** (30%). Compound **9** was identified by comparison with an authentic sample [40]; compound **10** was characterized spectroscopically (see below).

Data of N-[7-(Hexyloxy)-1,2-dihydro-2,2-diphenyl-3H-indol-3-ylidene]aniline (10). M.p. 100–101° (ligroin, b.p. 40–60°). IR: 1657(C=N), 1591(Ph–N(O–hexyl)–C). 1H -NMR (200 MHz, $CDCl_3$):

Table 5. X-Ray Diffraction Data for **3d** and **10**

Compound	3d	10
Formula	C ₃₂ H ₃₀ N ₂ O ₃	C ₃₂ H ₃₂ N ₂ O
<i>M_r</i>	490.6	460.6
Space group	<i>P2₁2₁2₁</i>	<i>Pbcn</i>
<i>a</i> [Å]	10.272(2)	38.136(6)
<i>b</i> [Å]	28.347(4)	7.2893(11)
<i>c</i> [Å]	9.056(2)	18.683(3)
α, β, γ [°]	90	90
<i>V</i> [Å ³]	2636.9(9)	5193.4(14)
<i>Z</i>	4	8
<i>T</i> [°C]	23(2)	25(2)
λ [Å]	1.54178	0.71073
ρ_{calc} [g cm ⁻³]	1.236	1.178
μ [cm ⁻¹]	6.30	0.71
Transmission coefficient	0.978–1.000	0.994–1.000
<i>R</i> ^a)	0.037	0.037
<i>wR</i> ₂	0.094	0.044
GOF	1.019	0.646
Observed refl.	3936	991
Independent refl. (<i>I</i> > 2σ(<i>I</i>))	4747	3734
Refined refl.	4747	3734
Variables	335	320

7.05–7.15 (*m*, 2 H); 7.27–7.41 (*m*, 10 H); 7.48–7.63 (*m*, 3 H). EI-MS (pos.): 461(2, *M*⁺), 260 (92.15), 384 (26), 383 (100), 299 (64), 221 (32), 167 (45), 165 (29), 77 (48). Anal. calc. for C₃₂H₃₂N₂O: C 83.44, H 7.0, N 6.08; found: C 84.41, H 7.15, N 6.18.

6. X-Ray Crystallography²⁾. 6.1. Compound **3d**. C₃₂H₃₀N₂O₃, *M_r* 490.6, orthorhombic, space group *P2₁2₁2₁*; *a* = 10.272(2), *b* = 28.347(4), *c* = 9.056(2) Å, *V* = 2636.9(9) Å³, *Z* = 4; ρ = 1.236 g cm⁻³; $\lambda(\text{CuK}\alpha)$ = 1.54178 Å, $\mu(\text{CuK}\alpha)$ = 6.30 cm⁻¹; colorless prism (0.14 × 0.15 × 0.20 mm). The structure was solved by direct methods (SIR97 [41]) and anisotropically refined for all non-H atoms. The H-atoms were located from a difference *Fourier* map and thereafter treated as riding atoms, the isotropic displacement parameter *U*_{iso}(H) set at 1.2 *U*_{eq}(C). The structure was refined on *F*² values (SHELX97 [42]) by using the weighting scheme $w = 1/[\sigma^2(F_o^2) + (0.0515 P)^2]$, where $P = (F_o^2 + 2 F_c^2)/3$. For 4747 unique reflections having *I* > 0 collected at *T* = 296(2) K on an *Enraf-Nonius CAD4* diffractometer (3 < 2θ < 140°), the final *R* value was 0.037 (*wR*₂ = 0.094; *S* = 1.019). See also Table 5.

6.2. Compound **10**. C₃₂H₃₂N₂O, *M_r* 460.6, orthorhombic, space group *Pbcn*; *a* = 38.136(6), *b* = 7.2893(11), *c* = 18.683(3) Å, *V* = 5193.4(14) Å³, *Z* = 8; ρ = 1.178 g cm⁻³; $\lambda(\text{MoK}\alpha)$ = 0.71072 Å, $\mu(\text{MoK}\alpha)$ = 0.71 cm⁻¹; yellow plate (0.03 × 0.09 × 0.15 mm). The structure was solved by direct methods (SIR 97 [41]) and anisotropically refined for all the non-H-atoms. The H-atom bound to N(1) was located from a difference *Fourier* map and refined isotropically. All other H-atoms were located from a difference *Fourier* map and thereafter treated as riding atoms, the isotropic displacement parameter *U*_{iso}(H) set at 1.2 *U*_{eq}(C) for Me H-atoms. The structure was refined on *F*² values (SHELX97 [42]) with the

²⁾ The crystallographic data of **3d** and **10** have been deposited with the *Cambridge Crystallographic Data Centre* as supplementary publication numbers CCDC-605374 and CCDC-605375, resp. Copies of the data can be obtained, free of charge, via the internet at http://www.ccdc.cam.ac.uk/data_request/cif.

weighting scheme $w = 1/[\sigma^2(F_o^2)]$. For 3734 unique reflections with $I > 0$ collected at 298(2) K on a *Bruker SMART CCD* diffractometer ($2.8 < 2\theta < 45.6^\circ$), the final R value was 0.037 ($wR_2 = 0.044$; $S = 0.646$). See also *Table 5*.

REFERENCES

- [1] D. H. Solomon, E. Rizzardo, P. Cacioli, US Pat. 4,581,429; Eur. Pat. Appl. 135280 (*Chem. Abstr.* **1985**, 102, 221335q).
- [2] M. K. Georges, R. P. N. Veregin, P. M. Kazmaier, G. K. Hamer, *Macromolecules* **1993**, 26, 2987.
- [3] C. J. Hawker, *Acc. Chem. Res.* **1997**, 30, 373.
- [4] C. J. Hawker, A. W. Bosman, E. Harth, *Chem. Rev.* **2001**, 101, 3661, and refs. cit. therein.
- [5] D. Greszta, K. Matyjaszewski, *Macromolecules* **1996**, 29, 7661, and refs. cit. therein.
- [6] H. Fischer, M. Souaille, *Chimia* **2001**, 55, 109.
- [7] T. Fukuda, A. Goto, K. Ohno, *Macromol. Rapid Commun.* **2000**, 21, 151.
- [8] H. Fischer, *Chem. Rev.* **2001**, 101, 3581, and refs. cit. therein.
- [9] A. Goto, T. Fukuda, *Prog. Polym. Sci.* **2004**, 29, 329, and refs. cit. therein.
- [10] T. Fukuda, A. Goto, Y. Tsujii, in 'Handbook of Radical Polymerization', Eds. K. Matyjaszewski, T. P. Davis, John Wiley & Sons, New York, 2002, p. 407, and refs. cit. therein.
- [11] H. Fischer, *ACS Symp. Ser.* **2003**, 854, 10.
- [12] K. Matyjaszewski, 'Controlled Radical Polymerization', American Chemical Society, Washington, DC, 1998, Vol. 685.
- [13] 'Controlled-Living Radical Polymerization: Progress in ATRP, NMP, and RAFT', Ed. K. Matyjaszewski, American Chemical Society, Washington, DC, 2000, Vol. 768.
- [14] K. Matyjaszewski, *Macromol. Symp.* **2001**, 174, 51.
- [15] G. Moad, E. Rizzardo, *Macromolecules* **1995**, 28, 8722.
- [16] S. Grimaldi, F. Le Moigne, J.-P. Finet, P. Tordo, P. Nicol, M. Plechot, Int. Pat. WO 96/24620, 15 August, 1996.
- [17] D. Benoit, V. Chiplinski, R. Braslau, C. J. Hawker, *J. Am. Chem. Soc.* **1999**, 121, 3904.
- [18] M.-O. Zink, A. Kramer, P. Nesvadba, *Macromolecules* **2000**, 33, 8106.
- [19] P. Nesvadba, M.-O. Zink, A. Kramer, DE 19909767, 1999 (*Chem. Abstr.* 131:229170).
- [20] J.-L. Couturier, O. Guerret, D. Gigmes, S. Marque, F. Chauvin, P.-E. Dufils, D. Bertin, P. Tordo, Pat. FR2843394, 2004; WO 2004014926.
- [21] C. Wetter, J. Gierlich, C. A. Knoop, C. Müller, T. Schulte, A. Studer, *Chem. – Eur. J.* **2004**, 10, 1156.
- [22] E. Drockenmüller, J.-M. Catala, *Macromolecules* **2002**, 35, 2461.
- [23] C. J. Hawker, in 'Handbook of Radical Polymerization', Eds. K. Matyjaszewski, T. P. Davis, J. Wiley & Sons, New York, 2002, p. 463, and refs. cit. therein.
- [24] D. Benoit, S. Grimaldi, S. Robin, J.-P. Finet, P. Tordo, Y. Gnanou, *J. Am. Chem. Soc.* **2000**, 122, 5929.
- [25] K. Matyjaszewski, *ACS Symp. Ser.* **2003**, 854, 2.
- [26] J. Nicolas, L. Mueller, J. Belleney, B. Charleux, *Macromolecules* **2005**, 38, 5485.
- [27] Y. Guillaneuf, P. Astolfi, D. Gigmes, S. R. A. Marque, P. Tordo, L. Greci, D. Bertin, *J. Am. Chem. Soc.*, submitted.
- [28] C. Berti, M. Colonna, L. Greci, L. Marchetti, *Tetrahedron* **1975**, 31, 1745.
- [29] A. Alberti, P. Carloni, L. Greci, P. Stipa, C. Neri, *Polym. Degrad. Stab.* **1993**, 39, 215.
- [30] E. Minaux, L. Greci, M. Buback, P. Tordo, T. Senninger, P. Stipa, P. Carloni, E. Damiani, G. Tommasi, EP Pat. 1120430, 2001.
- [31] K. Matyjaszewski, B. E. Woodworth, X. Zhang, S. Gaynor, Z. Metzner, *Macromolecules* **1998**, 31, 5955.
- [32] B. Witkop, J. B. Patrik, *J. Am. Chem. Soc.* **1951**, 73, 713.
- [33] D. R. Duling, *J. Magn. Reson., B* **1994**, 104, 105.
- [34] M. J. Frisch, G. W. Trucks, H. B. Schlegel, G. E. Scuseria, M. A. Robb, J. R. Cheeseman, J. A. Montgomery Jr., T. Vreven, K. N. Kudin, J. C. Burant, J. M. Millam, S. S. Iyengar, J. Tomasi, V. Barone, B. Mennucci, M. Cossi, G. Scalmani, N. Rega, G. A. Petersson, H. Nakatsuji, M. Hada, M. Ehara, K. Toyota, R. Fukuda, J. Hasegawa, M. Ishida, T. Nakajima, Y. Honda, O. Kitao, H. Nakai, M. Klene,

- X. Li, J. E. Knox, H. P. Hratchian, J. B. Cross, C. Adamo, J. Jaramillo, R. Gomperts, R. E. Stratmann, O. Yazyev, A. J. Austin, R. Cammi, C. Pomelli, J. W. Ochterski, P. Y. Ayala, K. Morokuma, G. A. Voth, P. Salvador, J. J. Dannenberg, V. G. Zakrzewski, S. Dapprich, A. D. Daniels, M. C. Strain, O. Farkas, D. K. Malick, A. D. Rabuck, K. Raghavachari, J. B. Foresman, J. V. Ortiz, Q. Cui, A. G. Baboul, S. Clifford, J. Cioslowski, B. B. Stefanov, G. Liu, A. Liashenko, P. Piskorz, I. Komaromi, R. L. Martin, D. J. Fox, T. Keith, M. A. Al-Laham, C. Y. Peng, A. Nanayakkara, M. Challacombe, P. M. W. Gill, B. Johnson, W. Chen, M. W. Wong, C. Gonzalez, J. A. Pople, Gaussian03, Revision C.02, *Gaussian, Inc.*, Wallingford CT, U.S.A., 2004.
- [35] A. Gaudel-Sri, D. Siri, P. Tordo, *ChemPhysChem* **2006**, *7*, 430.
- [36] E. R. Johnson, O. J. Clarkin, G. A. DiLabio, *J. Phys. Chem., A* **2003**, *107*, 9953; X.-Q. Yao, X.-J. Hou, H. Jiao, H.-W. Xiang, Y.-W. Li, *J. Phys. Chem., A* **2003**, *107*, 9991; Y. Feng, L. Liu, J.-T. Wang, H. Huang, Q.-X. Guo, *J. Chem. Inf. Comput. Sci.* **2003**, *43*, 2005.
- [37] M. W. Wong, *Chem. Phys. Lett.* **1996**, *256*, 391.
- [38] E. Janzen, B. J. Blackburn, *J. Am. Chem. Soc.* **1969**, *91*, 44; A. Ledwith, P. Russel, L. H. Sutcliffe, *Proc. R. Soc. A* **1973**, *151*, 332.
- [39] C. Rizzoli, P. Sgarabotto, F. Ugozzoli, P. Carloni, E. Damiani, L. Greci, P. Stipa, *J. Heterocycl. Chem.* **1993**, *30*, 637, and refs. cit. therein.
- [40] C. Berti, L. Greci, L. Marchetti, *J. Chem. Soc., Perkin Trans. 2* **1977**, 1032.
- [41] A. Altomare, M. C. Burla, M. Camalli, G. Cascarano, C. Giacovazzo, A. Guagliardi, A. G. G. Moliterni, G. Polidori, R. Spagna, *J. Appl. Crystallogr.* **1999**, *32*, 115.
- [42] G. M. Sheldrick, SHELXL97, University of Göttingen, Göttingen, 1997.

Received April 28, 2006